Cyclopentadienyl-Silyl-Amido versus Imido Niobium Complexes. The Role of Additional Amine Functionalities: A Combined Experimental and Theoretical Study†

M. Carmen Maestre,§ Marta E. G. Mosquera,‡,§ Heiko Jacobsen,⊥,¶ Gerardo Jiménez,*,§ and Tomás Cuenca*,§

Departamento de Química Inorgánica, Universidad de Alcalá, Campus Universitario, 28871 Alcalá de Henares, Spain, and Kemkom, Libellenweg 2, 25917 Leck, Nordfriesland, Germany

Received October 8, 2007

The reaction of the chlorosilyl-substituted cyclopentadienyl niobium compound [Nb(η^5-$C_5H_4SiMe_2Cl$)Cl_4] (**1**) with 1 equiv of propylenediamine or *N*-methylpropylenediamine in toluene in the presence of 2 equiv of NEt_3 affords the cyclopentadienyl-silyl-amido-amine derivatives [Nb{η^5-$C_5H_4SiMe_2$-η-$N(CH_2)_3$-η-NHR}Cl_3] (R = H, **3a**; Me, **3b**). In contrast, a similar reaction using the *N*,*N*-dimethylpropylene diamine regiospecifically yields the imido compound [Nb(η^5-$C_5H_4SiMe_2Cl$)-{$N(CH_2)_3NMe_2$}Cl_2] (**4a**). However, treatment of **1** with 3 equiv of *N*-methylpropylene diamine in the absence of NEt_3 gives the imido complex [Nb(η^5-$C_5H_4SiMe_2Cl$){$N(CH_2)_3NHMe$}Cl_2] (**4b**). The reaction of **1** with 0.5 equiv of $NH_2(CH_2)_3NH_2$ in the presence of 2 equiv of NEt_3 proceeds with the formation of the tethered dinuclear diimido compound [{Nb(η^5-$C_5H_4SiMe_2Cl$)Cl_2}$_2${μ-$N(CH_2)_3$-η-N}] (**5a**). Analogous dinuclear diimido compounds [{Nb(η^5-$C_5H_4SiMe_2Cl$)Cl_2}$_2${μ-$N(CH_2)_n$-η-N}] (n = 4, **5b**; 5, **5c**) are obtained when **1** reacts with longer unsubstituted diamines $NH_2(CH_2)_nNH_2$ (n = 4 and 5), regardless of the reaction proportions. The transient dinuclear diamine adducts of such a process, [{Nb(η^5-$C_5H_4SiMe_2Cl$)Cl_4}$_2${μ-$NH_2(CH_2)_n$-η-NH_2}] (n = 3, **6a**; 4, **6b**; 5, **6c**), have been prepared and isolated when these reactions were performed in the absence of a base. All compounds have been characterized by elemental analysis and NMR spectroscopy, and the crystal structures of the complexes [Nb{η^5-$C_5H_4SiMe_2$-η-$N(CH_2)_2NMe_2$}Cl_3] (**2c**) and [{Nb(η^5-$C_5H_4SiMe_2Cl$)Cl_4}(μ-$NH_2(CH_2)_4NH_2$)] (**6b**) have been determined by X-ray diffraction methods. The experimental work has been assisted by DFT calculations to determine the role played by the pendant amine group in this kind of process and the cause for the highfield shifted resonances for the cyclopentadienyl *ipso*-carbon in constrained-geometry complexes.

Introduction

Since Bercaw introduced the well-defined cyclopentadienyl-amido scandium complex [{Sc(η^5-$C_5Me_4SiMe_2$-η-N*t*Bu)-PMe_3}$_2$(μ-H)$_2$] in 1990 as an active olefin polymerization catalyst even in the absence of a cocatalyst,[1–3] there has been a continuous and increasing interest in the chemistry of transition-metal compounds bearing *ansa*-monocyclopentadienyl-amido ligands (constrained-geometry complexes, CGCs).[4–9] This field has largely been stimulated by the extensive use of the group 4 CGCs as alternative catalysts to the classical bis(cyclopentadienyl) systems[10–15] (MCp_2X_2) for α-olefin polymerization processes, due to their high activity and the unique properties of the polymers and copolymers obtained.[8,16,17] However, although several synthetic strategies have been developed to prepare cyclopentadienyl-amido group 4 metal complexes,[18] among which might be mentioned the reaction of the ligand precursor with a suitable metal compound via a

* Corresponding authors. Tel: 34918854655. Fax: 34918854683. E-mail: tomas.cuenca@uah.es, gerardo.jimenez@uah.es.

‡ Correspondence concerning the crystallography data should be addressed to this author. E-mail: martaeg.mosquera@uah.es.

† Dedicated to Professor Pascual Royo on the occasion of his 70th birthday.

§ Universidad de Alcalá.

⊥ Kemkom.

¶ Current address: Department of Chemistry, Tulane University, 6400 Freret St., New Orleans, LA 70118.

(1) Shapiro, P. J.; Bunel, E.; Schaefer, W. P.; Bercaw, J. E. *Organometallics* **1990**, *9*, 867–869.

(2) Shapiro, P. J.; Cotter, W. D.; Schaefer, W. P.; Labinger, J. A.; Bercaw, J. E. *J. Am. Chem. Soc.* **1994**, *116*, 4623–4640.

(3) Cano, J.; Kunz, K. *J. Organomet. Chem.* **2007**, *447*, 4411–4423.

(4) Okuda, J.; Eberle, T. Half-Sandwich Complexes as Metallocene Analogues. In *Metallocenes*; Togni A., H. R. L., Eds.; Wiley-VCH: New York, 1998; Vol. 1, Chapter 7.

(5) McKnight, A. L.; Waymouth, R. M. *Chem. Rev.* **1998**, *98*, 2587–2598.

(6) Britovsek, G. J. P.; Gibson, V. C.; Wass, D. F. *Angew. Chem., Int. Ed.* **1999**, *38*, 428–447.

(7) Gibson, V. C.; Spitzmesser, S. K. *Chem. Rev.* **2003**, *103*, 283–315.

(8) Kunz, K.; Erker, G.; Kehr, G.; Frohlich, R.; Jacobsen, H.; Berke, H.; Blacque, O. *J. Am. Chem. Soc.* **2002**, *124*, 3316–3326.

(9) Braunschweig, H.; Breitling, F. M. *Coord. Chem. Rev.* **2006**, *250*, 2691–2720.

(10) Jordan, R. F. *Adv. Organomet. Chem.* **1991**, *32*, 325–387.

(11) Marks, T. J. *Acc. Chem. Res.* **1992**, *25*, 57–65.

(12) Brintzinger, H. H.; Fischer, D.; Mülhaupt, R.; Rieger, B.; Waymouth, R. M. *Angew. Chem., Int. Ed. Engl.* **1995**, *34*, 1143–1170.

(13) Bochmann, M. *J. Chem. Soc., Dalton Trans.* **1996**, 255–270.

(14) Hlatky, G. G. *Coord. Chem. Rev.* **1999**, *181*, 243–296.

(15) Alt, H. G.; Koppl, A. *Chem. Rev.* **2000**, *100*, 1205–1221.

(16) Chum, P. S.; Kruper, W. J.; Guest, M. J. *Adv. Mater.* **2000**, *12*, 1759–1767.

(17) Lian, B.; Thomas, C. M.; Navarro, C.; Carpentier, J. F. *Organometallics* **2007**, *26*, 187–195.

(18) Cuenca, T. *Comprehensive Organometallic Chemistry III*; Mingos, M. P., Crabtree, R. H., Eds.; Bochmann, M., Vol. Ed.; Elsevier: London, 2006; Vol. 4, Chapter 5.

10.1021/om701003t CCC: $40.75
Publication on Web 02/05/2008

Scheme 1

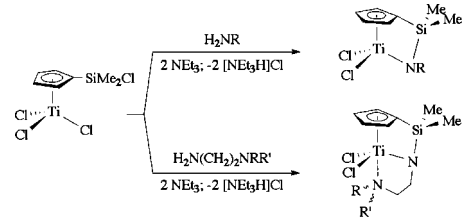

metathesis reaction using the dilithium salts[19,20] or amine/alkane elimination,[21–23] these have not been suitable synthetic approachs[24] to produce the labile cyclopentadienyl-silyl-amido group 5 metal derivatives.[25]

We have recently reported an efficient and versatile alternative strategy to prepare titanium cyclopentadienyl–amido derivatives based on the reaction of primary mono-[26–29] and diamines[30,31] with the chlorosilyl-substituted cyclopentadienyl compound $[Ti(\eta^5\text{-}C_5H_4SiMe_2Cl)Cl_3]$[32] in the presence of a base (NEt_3). Thus, reaction of $[Ti(\eta^5\text{-}C_5H_4SiMe_2Cl)Cl_3]$ with NH_2R (R = alkyl group, $(CH_2)_nNRR'$) specifically proceeds with the aminolysis of the Ti−Cl and Si−Cl bonds and the double deprotonation of the NH_2 amine group to render the corresponding cyclopentadienyl-silyl-amido derivative (Scheme 1).

We proposed to extend this synthetic methodology for the production of cyclopentadienyl-silyl-amido complexes of niobium by performing the parallel reactions with the analogous compound $[Nb(\eta^5\text{-}C_5H_4SiMe_2Cl)Cl_4]$[33] (**1**). In these reactions two different types of *N*-substituted niobium complexes were obtained depending on the nature of the amine employed. Whereas primary amines furnish the corresponding imido complexes,[34,35] ethylenediamines with at least a primary amine end, $H_2N(CH_2)_2NRR'$ (R = R′ = H, Me; R = H, R′ = Me), render cyclopentadienyl-silyl-amido-amine compounds (Scheme 2), signifying the importance of the pendant donor chain in reactions of this type.[36] Furthermore, in contrast to the characteristic lability found in the few examples of constrained-geometry niobium compounds reported,[25] a remarkable characteristic of complexes **2** is their notable photo and thermal stability.

Scheme 2

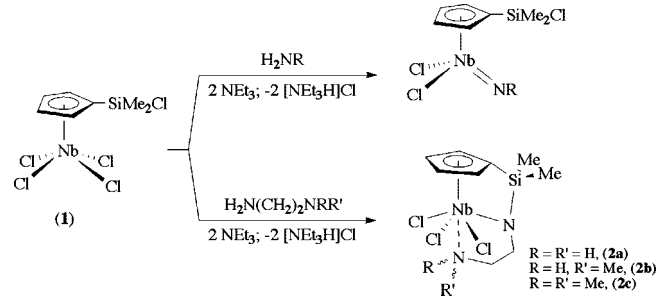

In view of such results, the presence of the pendant amine group is believed to play a critical role both in determining the course of the reaction and in stabilizing the cyclopentadienyl-silyl-amido-amine niobium complexes formed, from both an electronic and a steric point of view.

To support this proposal, we extend here the reactivity study of **1** with different primary organic diamines containing a longer chain, $NH_2(CH_2)_nNRR'$ ($n \geq 3$), and in different working conditions to evaluate the influence of the length of the connecting carbon chain and the effect of the different bases used on the nature of the final product obtained, a cyclopentadienyl-silyl-amido or an imido derivative. Moreover, the cyclopentadienyl-silyl-amido/imido dilemma and the reason for the highfield shifted resonances for the cyclopentadienyl *ipso*-carbon in CGCs have been approached by means of a computational chemistry study using DFT calculations.

Results

Reactions of $[Nb(\eta^5\text{-}C_5H_4SiMe_2Cl)Cl_4]$ (1) with Diamines $NH_2(CH_2)_nNRR'$ ($n \geq 3$). Treatment of **1** with 1 equiv of propylene- or *N*-methylpropylenediamine in toluene in the presence of 2 equiv of NEt_3 rendered the corresponding cyclopentadienyl-silyl-amido-amine derivative $[Nb\{\eta^5\text{-}C_5H_4SiMe_2\text{-}\eta\text{-}N(CH_2)_3\text{-}\eta\text{-}NHR\}Cl_3]$ (R = H, **3a**[36] Me, **3b**), isolated as analytically pure yellow solids in excellent yields. The reaction specifically proceeds with the aminolysis of the Nb−Cl and Si−Cl bonds and the double deprotonation of the NH_2 amine group, the same result as that obtained in the reaction of **1** with ethylenediamines.[36] However, when the parallel reaction was performed using the *N*,*N*-dimethylpropylenediamine the imido complex $[Nb(\eta^5\text{-}C_5H_4SiMe_2Cl)\{N(CH_2)_3NMe_2\}Cl_2]$ (**4a**) was obtained, as a pure green solid in high yield, as a consequence of the elimination of two HCl molecules by aminolysis of two Nb−Cl bonds, retaining the Si−Cl bond unreacted. This result contrasts with that achieved when the *N*,*N*-dimethylethylenediamine was used (see Scheme 2).[36]

When these reactions were carried out using an excess of diamine [1(Nb):3(diamine) molar ratio], in the absence of the NEt_3 (the diamine is itself used as base), the final results depend on the diamine employed. Thus, with the propylenediamine or the *N*,*N*-dimethylpropylenediamine the compounds **3a** and **4a** were obtained, whereas for the *N*-methylpropylenediamine the imido complex $[Nb(\eta^5\text{-}C_5H_4SiMe_2Cl)\{N(CH_2)_3NHMe\}Cl_2]$ (**4b**) was formed instead of the cyclopentadienyl-silyl-amido-amine complex **3b** (Scheme 3).

The different behavior observed in these reactions depending on the nature of the diamines (compared with the ethylenediamines and between the propylenediamines themselves) may

(19) Amor, F.; Okuda, J. *J. Organomet. Chem.* **1996**, *520*, 245–248.
(20) Dias, H. V. R.; Wang, Z. Y.; Bott, S. G. *J. Organomet. Chem.* **1996**, *508*, 91–99.
(21) Hughes, A. K.; Meetsma, A.; Teuben, J. H. *Organometallics* **1993**, *12*, 1936–1945.
(22) Herrmann, W. A.; Morawietz, M. J. A. *J. Organomet. Chem.* **1994**, *482*, 169–181.
(23) Chen, Y. X.; Marks, T. J. *Organometallics* **1997**, *16*, 3649–3657.
(24) Feng, S. G.; Roof, G. R.; Chen, E. Y. X. *Organometallics* **2002**, *21*, 832–839.
(25) Herrmann, W. A.; Baratta, W. *J. Organomet. Chem.* **1996**, *506*, 357–361.
(26) Ciruelos, S.; Cuenca, T.; Gómez, R.; Gómez-Sal, P.; Manzanero, A.; Royo, P. *Organometallics* **1996**, *15*, 5577–5585.
(27) Cuenca, T.; Royo, P. *Coord. Chem. Rev.* **1999**, *195*, 447–498.
(28) Gómez, R.; Gómez-Sal, P.; Martín, A.; Nuñez, A.; del Real, P. A.; Royo, P. *J. Organomet. Chem.* **1998**, *564*, 93–100.
(29) Gómez, R.; Gómez-Sal, P.; delReal, P. A.; Royo, P. *J. Organomet. Chem.* **1999**, *588*, 22–27.
(30) Jiménez, G.; Rodríguez, E.; Gómez-Sal, P.; Royo, P.; Cuenca, T.; Galakhov, M. *Organometallics* **2001**, *20*, 2459–2467.
(31) Jiménez, G.; Royo, P.; Cuenca, T.; Herdtweck, E. *Organometallics* **2002**, *21*, 2189–2195.
(32) Ciruelos, S.; Cuenca, T.; Gómez-Sal, P.; Manzanero, A.; Royo, P. *Organometallics* **1995**, *14*, 177–185.
(33) Alcalde, M. I.; Gómez-Sal, P.; Martín, A.; Royo, P. *Organometallics* **1998**, *17*, 1144–1150.
(34) Alcalde, M. I.; Gómez-Sal, M. P.; Royo, P. *Organometallics* **1999**, *18*, 546–554.
(35) Arteaga-Müller, R.; Sánchez-Nieves, J.; Royo, P.; Mosquera, M. E. G. *Polyhedron* **2005**, *24*, 1274–1279.
(36) Maestre, M. C.; Tabernero, V.; Mosquera, M. E. G.; Jiménez, G.; Cuenca, T. *Organometallics* **2005**, *24*, 5853–5857.

Scheme 3

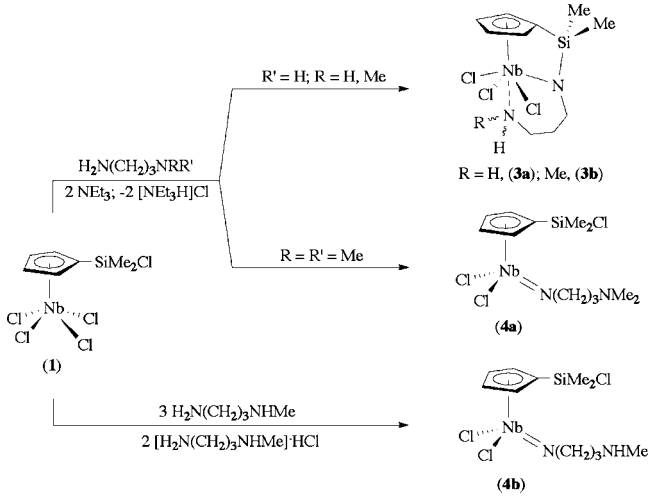

be based on the different ability of the second amine end to coordinate the metal center in an intramolecular manner. Such coordination capacity mainly depends on two structural factors of the diamines, the length of the hydrocarbon chain and the nature of the amine nitrogen substituents. The lengthening of the linking group, on going from a two- (in the ethylenediamines) to a three-carbon chain, causes the destabilization of the resulting metallacycle system resulting from the significant increase of the ring strain energy that the process involves. Rather, the contribution of the entropy effects is barely relevant, as inferred from the theoretical study.[37,38] In contrast, as the hydrocarbon spacer becomes longer, the diamine is more prone to coordinate to two rather than just one metal atom, probably as a result of decreased steric repulsion between the two metal-based molecular fragments.

Regarding the second structural factor, consistent with our finding,[39] a reduction in the number of hydrogen atoms at the amine nitrogen atom involves a decrease in the propensity of the amine group to coordinate. The origin of this effect might be attributed to both the decrease of the amine group nucleophilicity as the steric bulk of the amine substituents increases and the less pronounced ability to engage hydrogen bonding that may stabilize the N−Nb interactions.[40,41]

Hence, regarding the propylene- and the methylpropylenediamine, the higher tendency of the pendant amine group to coordinate outweighs the unfavorable effect of the increase in the ring strain in the resulting metalacycle. Consistently, the cyclopentadienyl-silyl-amido-amine complexes **3a** and **3b** are generated as a consequence of the intramolecular coordination of the pendant arm, similar to the reactions with ethylenediamines (see Scheme 2).[36] For the *N*,*N*-dimethylpropylenediamine, a combination of both unfavorable factors are produced, a longer linking chain and bulkier amine substituents, preventing the intramolecular coordination of the amine end. Thus, the formation of the imido derivative **4a** requires that in the course of such a reaction the pendant amine group NMe_2 remains uncoordinated to the niobium atom, behaving as a primary monoamine and rendering the same type of final compound.[34,35]

Scheme 4

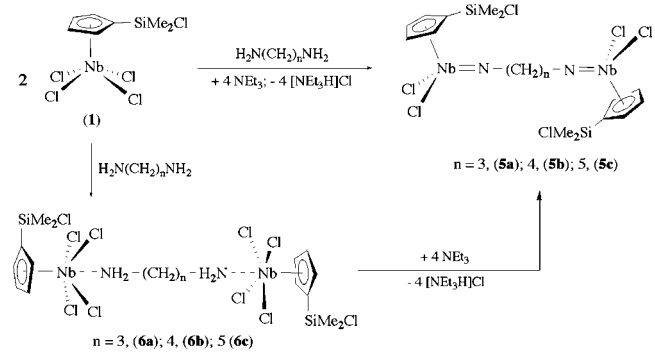

The different results obtained in the reactions with *N*-methylpropylenediamine (in the presence of NEt_3 or an excess of diamine) may be attributed to the coordinating ability of the different amine functionalities (NEt_3, NH_2, or NHMe). As a distinct form occurring with the NEt_3, the presence of free diamine results in a more pronounced ability to coordinate to the NH_2 unit, and the aminolysis process takes place on the NH_2 amine extreme with the pendant amine fragment NHMe displaced from the metal center, therefore forcing the formation of the imido compound.

Treatment of **1** with longer unsubstituted diamines $NH_2(CH_2)_nNH_2$ (n = 4, 5), as expected, never yielded the corresponding mononuclear cyclopentadienyl-silyl-amido-amine derivatives, regardless of the molar ratio of the diamine used. In all cases, the reaction of **1** with butylene and pentylene diamine rendered the dinuclear μ-diimido compounds [{Nb(η^5-$C_5H_4SiMe_2Cl$)Cl_2}$_2${μ-N(CH_2)$_n$-η-N}] (n = 4, **5b**; 5, **5c**) (Scheme 4), which were conveniently isolated after work-up as pure substances in high yields. Upon increase in the hydrocarbon chain length, the intramolecular coordination of the pendant amine group is hindered as a consequence of the lower stability of the potential chelate ring that might be formed, driving the process toward the formation of the imido derivative. In addition, after coordination of one of the NH_2 groups, the second NH_2 functionality is located far away, favoring contact with a second metal center and justifying the formation of only dinuclear complexes.

In view of the results discussed above and those obtained with the analogous titanium complex,[31] we decided to study the reaction of **1** with the propylenediamine in a 1(Nb):0.5(diamine) molar ratio. Thus, the reaction of **1** with 0.5 equiv of $NH_2(CH_2)_3NH_2$ in the presence of 2 equiv of NEt_3 selectively gave rise to the corresponding tethered dinuclear μ-diimido compound [{Nb(η^5-$C_5H_4SiMe_2Cl$)Cl_2}$_2${μ-N(CH_2)$_3$-η-N}] (**5a**) as an analytically pure substance (Scheme 4). The formation of **5a** under these reaction conditions shows that the process proceeds via intermolecular coordination and contrasts with the result achieved with the ethylenediamine, for which the formation of the analogous dinuclear imido derivative has been never observed. Such different behavior may be explained by assuming that, upon halving the amount of the diamine, the propylenediamine shows a lower propensity to coordinate in an intramolecular manner, which makes intermolecular coordination a more favorable energetic situation. This observation is in agreement with the conclusions obtained from the theoretical analysis.

When **1** was reacted with $NH_2(CH_2)_nNH_2$ in the absence of NEt_3, the formation of dinuclear adducts [{Nb(η^5-$C_5H_4SiMe_2Cl$)Cl_4}$_2$(μ-$NH_2(CH_2)_nNH_2$)] (n = 3, **6a**; 4, **6b**; 5, **6c**) was observed (Scheme 4). An unidentified solid precipitated over the course of the reaction, and the final compounds **6** were

(37) Hancock, R. D.; Martell, A. E. *Chem. Rev.* **1989**, *89*, 1875–1914.
(38) Boyd, C. L.; Clot, E.; Guiducci, A. E.; Mountford, P. *Organometallics* **2005**, *24*, 2347–2367.
(39) Maestre, M. C.; Paniagua, C.; Herdtweck, E.; Mosquera, M. E. G.; Jiménez, G.; Cuenca, T. *Organometallics* **2007**, *26*, 4243–4251.
(40) Fric, H.; Puchberger, M.; Schubert, U. *J. Sol-Gel Sci. Technol.* **2006**, *40*, 155–162.
(41) Fric, H.; Puchberger, M.; Schubert, U. *Eur. J. Inorg. Chem.* **2007**, 376–383.

Scheme 5

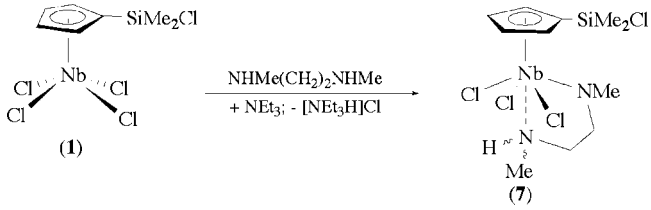

obtained as pure solids in lower than 50% yield. Nevertheless, once these complexes were isolated, they were quantitatively (as seen by NMR spectroscopy) converted to the corresponding dinuclear imido compound by treatment with 4 equiv of NEt_3, showing that the first reaction step is the coordination of the diamine to the niobium center. In addition, it also proves that the longer the diamine chain is, the more favorable the intermolecular coordination is, as confirmed by the theoretical study.

In trying to clarify the mechanism of these processes, we explored the reaction of **1** with *N*,*N*′-dimethylethylenediamine, which yields the amido-amine complex [Nb(η^5-$C_5H_4SiMe_2Cl$)(NMe$(CH_2)_2$-η-NHMe)Cl_3] (**7**) in good yield (Scheme 5). Compound **7** is isostructural with those compounds obtained in our research group by reaction of the ethylenediamine with monocyclopentadienyl compounds of niobium without a $SiMe_2Cl$ substituent at the ring, in which the expected imido derivative [NbCp(N$(CH_2)_2$NRR′)Cl_2] was never observed.[39] The combination of these results suggests that the second reaction step is the aminolysis of an Nb−Cl bond to form a transient amido similar to complex **7**, which can be stabilized with respect to the cleavage of a second Nb−Cl bond by coordination of the amine end.

All of these complexes were fully characterized by NMR spectroscopy and by elemental analysis. In addition, the X-ray molecular structures of the complexes [Nb{η^5-$C_5H_4SiMe_2$-η-N$(CH_2)_2NMe_2$}Cl_3][36] (**2c**) and [{Nb(η^5-$C_5H_4SiMe_2Cl$)Cl_4}$_2$(μ-$NH_2(CH_2)_4NH_2$)] (**6b**) are reported.

The ^{1}H NMR spectra of **3a**, **4a**, and **4b** feature AA′BB′ spin systems for the C_5H_4 ring protons, one signal for the SiMe_2 resonances, and three multiplets for methylene protons of the NCH_2CH_2CH_2NRR′ moiety in agreement with C_s symmetry of these molecules in solution. The ^{1}H NMR spectra of **3b** and **7** show an ABCD spin system for the C_5H_4 ring protons and two signals for the methyl groups on the silicon atom aside from a diasterotopic splitting of the methylene protons of the bridging fragment NCH_2CH_2CH_2NHMe or NCH_2CH_2NHMe. These NMR features are consistent with chiral species, which stem from the rigid coordination of the pendant amine functionality, thus preventing racemization at the amine nitrogen, as well as the different nature of the amine substituents that make the nitrogen atom become a stereogenic center. Such a bonding interaction is also proposed for **3a**, based on the pronounced downfield shift of the amine protons with respect to that found for the free amine. In contrast, the C_s symmetry shown for **4b** in solution and the high shift resonances for the amine protons observed in the ^{1}H NMR spectrum of this compound rule out the intramolecular coordination of the amine end in the imido complexes **4**.

Suitable ^{1}H NMR data to distinguish whether the chlorine atom initially on the silicon center remains bonded to silicon or reacts are the chemical shifts of the methyl groups on silicon (SiMe_2X) as such resonances depend notably on the nature of the X group. Thus, the SiMe_2N resonances ($\delta_{av} \approx 0.04$ in C_6D_6 and 0.51 in $CDCl_3$) in the cyclopentadienyl-silyl-amido derivatives appear highfield shifted (≈ 0.50 ppm in C_6D_6 and ≈ 0.20 ppm in $CDCl_3$, respectively) with respect to those found for the SiMe_2Cl unit in the imido compounds ($\delta_{av} \approx 0.55$ in C_6D_6 and 0.73 in $CDCl_3$) and the amido-amine derivative **7**. Nevertheless, the definitive NMR data to unambiguously establish the cyclopentadienyl-silyl-amido or imido nature of **3** and **4**, respectively, are the chemical shifts of the resonance due to the cyclopentadienyl *ipso*-carbon atom observed in the ^{13}C NMR spectra and the silicon resonances in the ^{29}Si NMR spectra (see theoretical study below).[25,36] In this regard, the constrained geometry for complex **3** is confirmed by the upfield shifted resonances for the cyclopentadienyl *ipso*-carbon with respect to the rest of the ring carbon atoms and the upfield shifted resonances for the silicon atoms (average value, −15 ppm) compared with those observed for the chlorosilyl-substituted cyclopentadienyl niobium compounds **4** and **7** (average value, 16 ppm).[33]

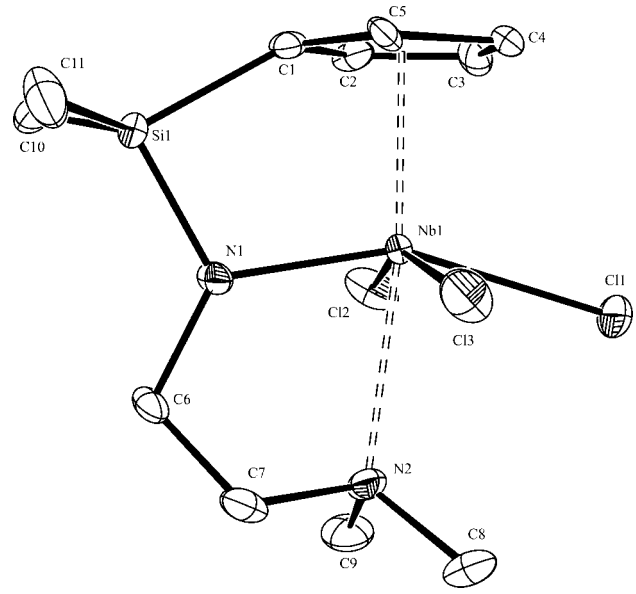

Figure 1. Molecular structure of **2c**, shown with 30% thermal ellipsoids. Hydrogen atoms are omitted for clarity.

The NMR spectroscopic behavior of **5** and **6** is relatively simple and consistent with the anticipated dinuclear structure. One singlet for the SiMe_2 resonances and one AA′BB′ spin systems for the C_5H_4 ring protons indicate that these compounds consist of two spectroscopically equivalent C_s-symmetric metallic units, Nb(η^5-$C_5H_4SiMe_2Cl$)(=N−)Cl_2 and Nb(η^5-$C_5H_4SiMe_2Cl$)(NH_2−)Cl_2, respectively, tethered by a carbon chain. The resonances assigned to the methylene protons of the hydrocarbon spacer appear as a set of multiplets with an integration ratio 4:2 for **5a** and **6a**; 4:4 for **5b** and **6b**; 4:4:2 for **5c** and **6c**. In addition, the chemical shifts of the methyl groups on silicon confirm the presence of the $SiMe_2Cl$ group in the cyclopentadienyl ring. The downfield shift of both the *ipso*-carbon atom and the silicon atom resonances in the ^{13}C NMR and the ^{29}Si NMR spectra confirm the imido and amine structure of these complexes.

Structural Studies. The molecular structure of [Nb{η^5-$C_5H_4SiMe_2$-η-N$(CH_2)_2NMe_2$}Cl_3][36] (**2c**) is illustrated in Figure 1 and selected bond distances and angles are listed in Table 1. The coordination geometry around the niobium center resembles that found in the analogous complex [Nb{η^5-$C_5H_4SiMe_2$-η-N$(CH_2)_3$-η-NH_2}Cl_3] (**3a**),[36] with the tridentate η^5-$C_5H_4SiMe_2$-η-N$(CH_2)_2$-η-NMe_2 ligand adopting a *mer*-disposition and the amine nitrogen located virtually *trans* to the cyclopentadienyl

Table 1. Selected Interatomic Distances (Å) and Angles (deg) for Complexes 2c and 6b[a]

Compound 2c			
Nb(1)−N(1)	1.996(2)	C(6)−N(1)−Si(1)	123.8(2)
Nb(1)−Cl(2)	2.484(3)	C(6)−N(1)−Nb(1)	125.71(18)
Nb(1)−Cl(1)	2.4854(9)	Si(1)−N(1)−Nb(1)	110.31(12)
Nb(1)−Cl(3)	2.488(3)	C(8)−N(2)−C(7)	108.8(6)
Nb(1)−N(2)	2.515(3)	C(8)−N(2)−C(9)	104.7(4)
N(1)−C(6)	1.482(4)	C(7)−N(2)−C(9)	107.7(5)
N(1)−Si(1)	1.762(2)	C(7)−N(2)−Nb(1)	102.4(3)
N(2)−C(8)	1.483(8)	C(8)−N(2)−Nb(1)	116.3(4)
N(2)−C(7)	1.497(6)	C(9)−N(2)−Nb(1)	116.6(5)
N(2)−C(9)	1.507(11)	C(7)−C(6)−N(1)	108.7(4)
Nb(1)−Cg	2.150	C(6)−C(7)−N(2)	112.7(5)
C(6)−C(7)	1.457(7)	Cg−Nb(1)−N(2)	172.99
		Cg−Nb(1)−N(1)	99.68
Compound 6b			
Nb(1)−N(1)	2.340(3)	N(1)−Nb(1)−Cl(4)	79.79(7)
Nb(1)−Cg	2.144	Cl(4)−Nb(1)−Cl(3)	154.54(3)
Nb(1)−Cl(2)	2.4306(9)	Cl(2)−Nb(1)−Cl(3)	85.47(3)
Nb(1)−Cl(3)	2.4481(10)	N(1)−Nb(1)−Cl(2)	77.42(8)
Nb(1)−Cl(4)	2.4266(9)	Cg−Nb(1)−N(1)	177.32
Nb(1)−Cl(5)	2.4388(9)	N(1)−C(1)−C(2)	113.8(3)
N(1)−C(1)	1.494(5)	C(1)−N(1)−Nb(1)	126.2(2)
C(2)−C(1)	1.553(5)		
C(2)−C(2)#1	1.488(8)		

[a] Cg denotes the centroid of the Cp ligand (symmetry transformations used to generate equivalent atoms: #1 $-x+2, -y+1, -z+2$).

group. In addition, the Cg(1)−Nb(1)−N(1) (Cg = centroid of the Cp ring) bond angle of 99.68° is comparable to the angles reported for the niobium CGCs [Nb{η^5-$C_5H_4SiMe_2$-η-$N(CH_2)_3$-η-NH_2}Cl_3][36] (100.98°) and [Nb(η^5-$C_5H_4SiMe_2$-η-NAr)(NAr)Cl][35] (100.76°), being more acute than those reported for unbridged amido ligands (106.60−116.67° range).[42]

However, analysis of the structural data indicates that the structural consequences of a decrease of one unit in the amido-amine spacer, on going from **3a** to **2c**, are significant. Thus, the structural parameters provide evidence that the five-membered ring present in **2c** is less strained than the **3a** six-membered ring, as the bond-angle values of the linker moiety $N(CH_2)_2$-η-NMe_2 in **2c** are closer to ideal values. As such, the environment around the N(1) atom in **2c** shows values nearer to the ideal figures for a planar geometry (110.31(12)°, 123.8(2)°, and 125.71(18)°) than in **3a** (108.44(11)°, 116.09(18)°, and 134.54(19)°). The disparity from ideal values is especially noticeable for **3a** in the environment of the extra carbon atom within the linker unit, which shows a most distorted tetrahedral geometry (N(1)−C(6)−C(7) 116°); also, the angle Nb(1)−N(1)−C(6) widens (134.54(19)°) to accommodate this extra carbon atom.

In contrast, though the Nb−N(1) bond distance (1.996(2) Å) is similar to that found in **3a** and comparable to those Nb−N bonds with an appreciable multiple bond character (1.935–2.102 Å),[43] the Nb−N(2) distance of 2.515(3) Å is notably longer than in **3a** and is one of the longest reported (Nb−N bond range 1.93–2.51 Å),[44–47] such elongation also contributes to minimizing the strain in the metallacycle. The angles around N(2) are close to the ideal values expected for tetrahedral geometry and are consistent with sp^3 hybridization.

Single-crystal X-ray diffraction (Figure 2) of **6b** confirms the coordination of the diamine ligand bridging two niobium atoms. The molecular structure shows a dinuclear species with both metallic moieties connected by a $NH_2(CH_2)_4NH_2$ chain shaped in a crank shaft fashion, in which the two fragments are related by an inversion center. Interestingly, this compound is the first example where two niobium centers are linked by a primary diamine. As such, most of the derivatives where two transition metals were linked by the diamine $NH_2(CH_2)_4NH_2$ occur mainly in metals from groups 10–12. In particular, for group 5 very few multinuclear derivatives of vanadium have been characterized bearing the moiety M-$NR_2(CH_2)_nR_2$N-M (n = 1–4)[48,49] and none have been reported for niobium.

The niobium atoms are in a pseudo-octahedral environment with the chlorine atoms placed in the equatorial positions, whereas the apical positions are occupied by the cyclopentadienyl ring and the NH_2 group. The two sets of Cl atoms bonded to the Nb centers show an eclipsed disposition, while the two $SiMe_2Cl$ substituents in the Cp rings (one for each Nb atom) are orientated in opposite directions.

Around the niobium center, Nb−Cl distances (2.4266(9) Å to 2.4481(10) Å) are within the range for these kind of bonds. In addition, Nb(1)−N(1) (2.340(3) Å) falls within the range for single bonds (2.20–2.51 Å),[20] accordingly, the nitrogen atom shows a tetrahedral geometry as expected for a sp^3 hybridation.

In the molecular packing, the molecules are ordered along the *a* axis with their carbon chains parallel to each other. The structure is supported by intermolecular C-H···Cl weak hydrogen bonds.

Theoretical Study

To clarify and understand the results obtained in the treatment of the tetrachloro dimethylchlorosilyl-cyclopentadienyl niobium compound **1** with primary mono- and diamines under different reaction conditions,[36] a theoretical investigation based on density functional theory has been carried out. Our computational study focuses on the structures and energetics of gas-phase model scenarios, from which arguments for the different chemistry displayed by the different amines are derived.

Formation of an Initial Amido Complex. In Scheme 6, reaction enthalpies ΔH at 0 K and free energies of reaction ΔG at 298 K (values in kJ/mol) are reported for the reaction of **1** with ammonia and ethylenediamine to yield the amido complexes **Ia** and **Ib**, respectively.

Both transformations constitute endothermic processes; the formation of **Ib** is slightly more favorable in terms of enthalpy and free energy than the formation of **Ia**. However, the reactions are carried out in toluene in the presence of a surplus of amines NR_3, which capture the hydrochloric acid that is generated in the aminolysis process. Thus, HCl is effectively converted into the ammonium chloride salt $[NR_3H]Cl$, which precipitates out of the toluene solution. It is proposed that formation of this insoluble salt provides the thermodynamic driving force for the reaction. This argument also applies to other reaction steps that involve elimination of HCl (vide infra).

(42) Humphries, M. J.; Green, M. L. H.; Douthwaite, R. E.; Rees, L. H. *J. Chem. Soc., Dalton Trans.* **2000**, 4555–4562.
(43) Humphries, M. J.; Green, M. L. H.; Leech, M. A.; Gibson, V. C.; Jolly, M.; Williams, D. N.; Elsegood, M. R. J.; Clegg, W. *J. Chem. Soc., Dalton Trans.* **2000**, 4044–4051.
(44) Chesnut, R. W.; Fanwick, P. E.; Rothwell, I. P. *Inorg. Chem.* **1988**, *27*, 752–754.
(45) Jayaratne, K. C.; Yap, G. P. A.; Haggerty, B. S.; Rheingold, A. L.; Winter, C. H. *Inorg. Chem.* **1996**, *35*, 4910–4920.
(46) Corbin, R. A.; Dusick, B. E.; Phomphrai, K.; Fanwick, P. E.; Rothwell, I. P. *Chem. Commun.* **2005**, 1194–1196.
(47) Cotton, F. A.; Shang, M. Y. *J. Cluster Sci.* **1994**, *5*, 467–479.
(48) Tripathi, A.; Hughbanks, T.; Clearfield, A. *J. Am. Chem. Soc.* **2003**, *125*, 10528–10529.
(49) Hegetschweiler, K.; Morgenstern, B.; Zubieta, J.; Hagrman, P. J.; Lima, N.; Sessoli, R.; Totti, F. *Angew. Chem., Int. Ed.* **2004**, *43*, 3436–3439.

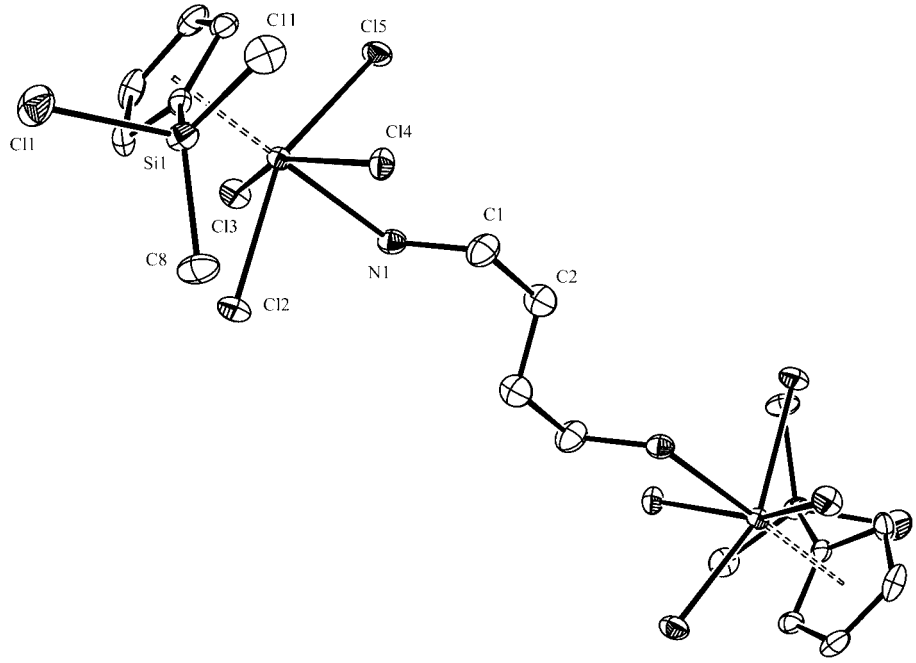

Figure 2. Molecular structure of **6b**, shown with 30% thermal ellipsoids. Hydrogen atoms are omitted for clarity.

Scheme 6

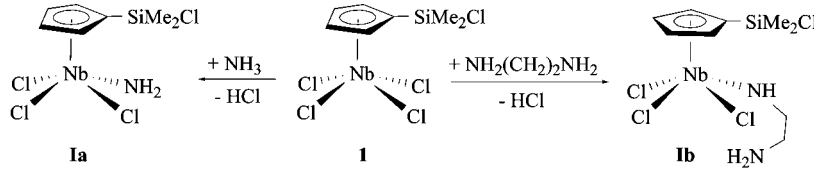

	Ia	**1**	**Ib**
ΔH(0K)	36	0	16
ΔG(298K)	44	0	29

Scheme 7

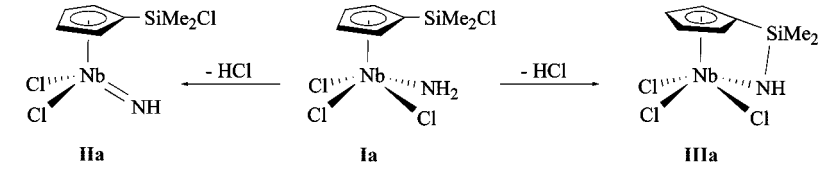

	IIa	**Ia**	**IIIa**
ΔH(0K)	80	0	90
ΔG(298K)	41	0	55

Formation of the Final Imido and Cyclopentadienyl-Silyl-Amido Complexes. The elimination of a second molecule of HCl initiates the generation of the final imido and cyclopentadienyl-silyl-amido complexes (Schemes 7 and 8).

Evaluating the energetics for complex **Ia** (Scheme 7), both the formation of the imido complex **IIa** and the cyclopentadienyl-silyl-amido compound **IIIa** constitute an endothermic reaction (as suggested above). In terms of free energy, formation of the imido complex **IIa** is calculated to occur with an energetic preference of about 15 kJ/mol over the formation of the amido compound **IIIa**. Formation of **IIa** takes place under HCl elimination incorporating a niobium-bonded chloro ligand, whereas formation of **IIIa** involves cleavage of the Si−Cl bond and generation of a N−Si linkage.

The same qualitative trends are found for imido and cyclopentadienyl-silyl-amido complexes **IIb** and **IIIb** that originate from complex **Ib** (Scheme 8). Again, the imido complex **IIb** is energetically favored over the cyclopentadienyl-silyl-amido compound **IIIb** by 33 kJ/mol (ΔH) and 47 kJ/mol (ΔG). Compared to products arising from complex **Ia**, the preference for the imido complex **IIb** is even more pronounced.

However, complexes **Ib**, **IIb**, and **IIIb** might be substantially stabilized by intramolecular donor stabilization of the niobium center by the additional amine group, resulting in the formation of amido complexes **IVb** and **Vb** and imido complex **VIb**. Compared to endothermic formation of the imido and amido complexes **IIb** and **IIIb**, formation of the intramolecular donor adduct **IVb** constitutes an exothermic process. It is therefore likely that the formation of **IIb** and **IIIb** is initiated by intramolecular donor stabilization.

Compared to reactants **I** and NR_3, only formation of the donor-stabilized amido complex **Vb** constitutes an exothermic ($\Delta H = -23$ kJ/mol) as well as an exergonic ($\Delta G = -55$ kJ/mol) reaction; the formation of the donor-stabilized imido complex **VIb** is an endothermic ($\Delta H = 72$ kJ/mol) as well as an endergonic ($\Delta G = 30$ kJ/mol) process.

The additional donor stabilization by intramolecular coordination of the additional amine group provides a rationale for the

Scheme 8

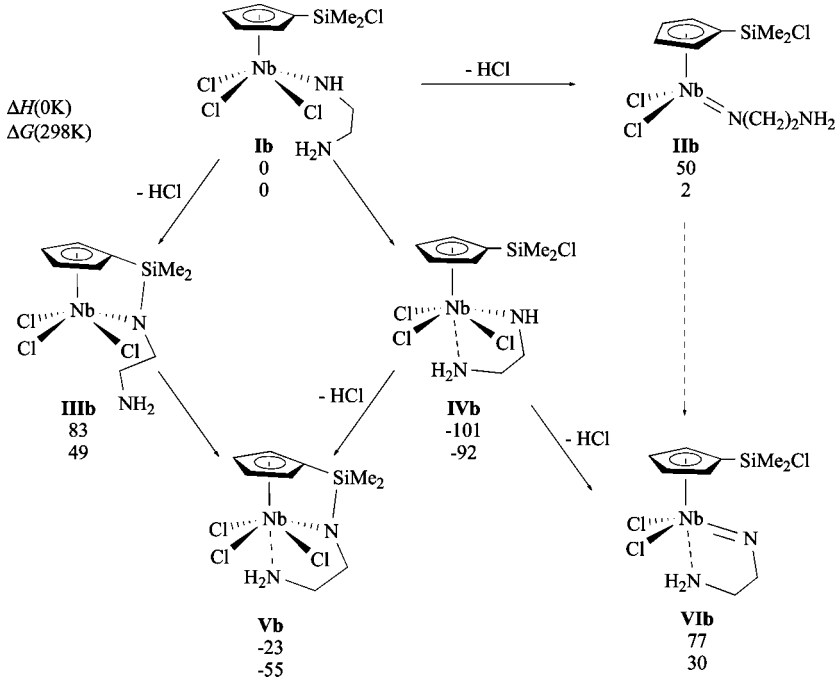

fact that reaction of **1** with diamines preferably yields cyclopentadienyl-silyl-amido complexes rather than imido compounds.

In Figure 3 the optimized geometries for complexes **IVb**, **Vb**, and **VIb** are displayed. Of special interest is the geometry of the five-membered metallacycle formed by the niobium atom and the chelating amido-amine and imido-amine ligands. Both amido complexes **IVb** and **Vb** show similar Nb−N(amido) distances (2.02 and 2.05 Å, respectively), and compound **VIb** displays a shorter N−Nb contact of 1.81 Å, indicating the double bond character of the metal−nitrogen linkage. Considering the value of the Nb−N−C angles around the amido or imido nitrogen, we find that the values for **IVb** and **Vb**, 124° and 123°, respectively, are close to the ideal value for an sp^2 hybridization. The Nb−N−C angle around the imido center in **VIb** amounts to 134° and is greatly distorted compared to the uncoordinated compound **IIb** (∠(Nb−N−C) = 171°). In addition, the distance between the amine group and the transition metal center in **VIb** is significantly larger by about 0.1 Å, suggesting a weaker donor interaction for the imido complex. The distortion of the coordination geometry of the imido nitrogen and the marked weakening of the Nb−N(imido) interaction together with a weaker donating interaction of the amine nitrogen justify the idea that the imido complex **IIb** is not stabilized by additional coordination of the pendant amine group.

Intermolecular Donor Stabilization. Since intramolecular donor stabilization is the decisive factor that favors formation of amido complex **IIIb** over imido complex **IIb**, the energetics of intermolecular donor stabilization have been alternatively evaluated (Scheme 9). All three complexes **Ia**, **IIa**, and **IIIa** are calculated to form stable complexes with ammonia. The calculated enthalpies for complex formation range from 44 to 103 kJ/mol. It is noteworthy that the imido complex **IIa** shows the weakest interaction with an additional donor ligand. It is not the fact that imido complexes do not undergo stabilizing interactions with additional donor ligands that favors formation of **Vb** over formation of **IIb** or **VIb**. However, this interaction is markedly weak, and when we further consider the distortion energy required for the imido ligand in **IIb** to adopt a chelating geometry, the process of intramolecular donor stabilization of imido complexes appears to be energetically unfavorable.

Intramolecular Donor Stabilization and Dinuclear Complexes. We have found that, depending of the length of the hydrocarbon spacer of $NH_2(CH_2)_nNH_2$ diamines, formation of dinuclear complexes is favored over intramolecular donor stabilization for ligands in which the amine groups are separated by three or more carbon centers. We have proposed that increasing the hydrocarbon chain length causes an increase in the ring strain in the resulting metalacycle and therefore induces formation of dinuclear complexes.

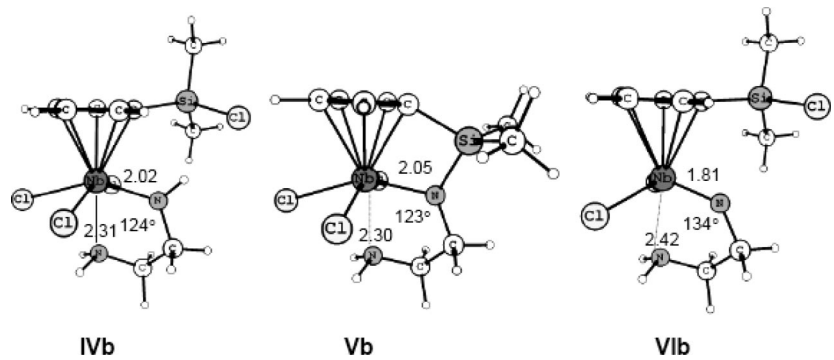

Figure 3. Optimized geometries for complexes **IVb**, **Vb**, and **VIb** together with selected bond distances (in Å) and bond angles.

Scheme 9

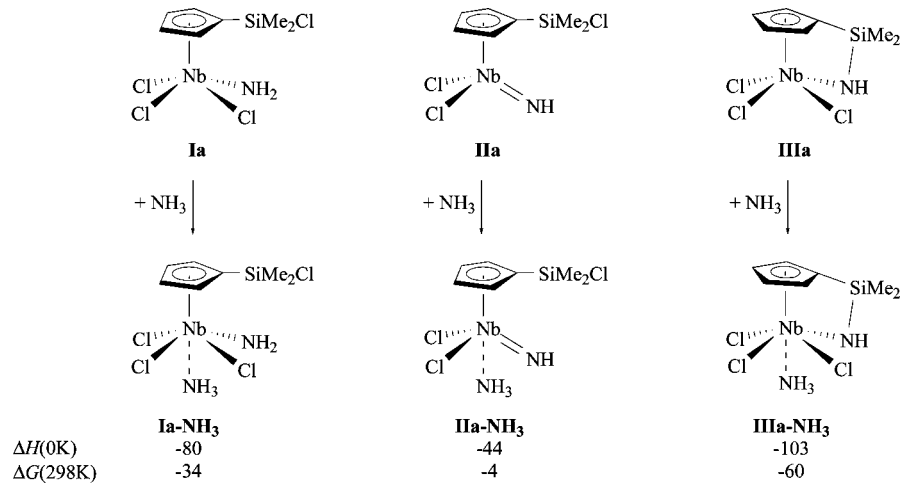

	Ia-NH_3	IIa-NH_3	IIIa-NH_3
ΔH(0K)	-80	-44	-103
ΔG(298K)	-34	-4	-60

Scheme 10

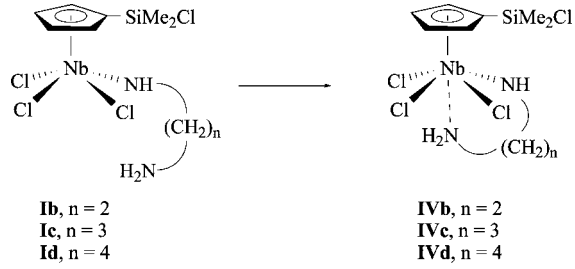

Table 2. Thermodynamic Properties (at 298K, kJ/mol) for Intramolecular Donor Stabilization

	x	ΔH	ΔG	$-T\Delta S$	$E_{\text{ring-strain}}$	E(N → Nb)
Ix → IVx	**b**, $n = 2$	−101	−92	9	37	−138
	c, $n = 3$	−87	−71	16	56	−143
	d, $n = 4$	−60	−43	17	75	−135

To validate our hypothesis, we performed additional calculations for [Nb(η^5-$C_5H_4SiMe_2Cl$)$Cl_3NH(CH_2)_3NH_2$] **Ic** and [Nb(η^5-$C_5H_4SiMe_2Cl$)$Cl_3NH(CH_2)_4NH_2$] **Id** (Scheme 10). Calculated thermodynamic properties for intramolecular donor stabilization are collected in Table 2.

As expected, the enthalpy as well as the free energy of intramolecular donor stabilization decreases with increasing length of the hydrocarbon spacer. However, the energetic contribution due to entropy, $-T\Delta S$, remains approximately the same and independent of the length of the hydrocarbon chain. Entropy effects are clearly not responsible for the fact that different diamines undergo intramolecular donor interactions of different strengths. To estimate the ring strain energy, we performed single point energy calculations on donor-disabled model complexes. These complexes were obtained by replacing the amine group in complexes of type **I** and **IV** by a hydrogen atom, and the enthalpy difference between complexes of type **I** and **IV** serves as a measure for the ring strain energy ($E_{\text{ring-strain}}$). $E_{\text{ring-strain}}$ increases from 37 kJ/mol for **IVb** to 75 kJ/mol for **IVd**. It is clearly the ring strain energy only that is responsible for the different coordination chemistry exhibited by different diamines. An estimate for the N → Nb bonding energy can be obtained as E(N → Nb) = $\Delta H - E_{\text{ring-strain}}$. All three complexes display a similar N → Nb bond energy of about −140 kJ/mol. The slighter lower E(N → Nb) energy for **IVd** reflects the slightly elongated Nb−N distance in the optimized complex.

We further estimated reaction enthalpies for formation of dinuclear amine-adducts as illustrated in Scheme 11.

Complexes **Ic** and **Id** with a propylamine and butylamine group bind to a free complex **1** with the same enthalpy of adduct formation. However, the bond enthalpy of complex **Ib** with an ethylamine group is 18 kJ/mol weaker compared to the analogues with a longer hydrocarbon spacer. This decrease in bond enthalpy is most likely due to increased steric repulsion between the two metal-based molecular fragments. We further note that for complex **Ib** intramolecular donor stabilization is more exothermic than formation of the dinuclear complex, whereas complexes **Ic** and **Id** display a reversed preference. It is now the formation of the dinuclear complex that is favored in terms of enthalpy. Since the formation of amido and imido complexes is initiated by adduct formation of a free amine functionality to a niobium center, this observation provides a rationale for the different chemistry of various diamine ligands as observed in the experiment.

Electronic Structure. A frontier orbital diagram for compounds **Vb** and **VIb** is displayed in Figure 4. For compound **VIb** without a N−Si bond, the major contribution to the HOMO/LUMO set stems from the lone pair π-orbital of the amido nitrogen, which interacts with the transition metal center in bonding and in antibonding fashion, respectively. Close in

Scheme 11

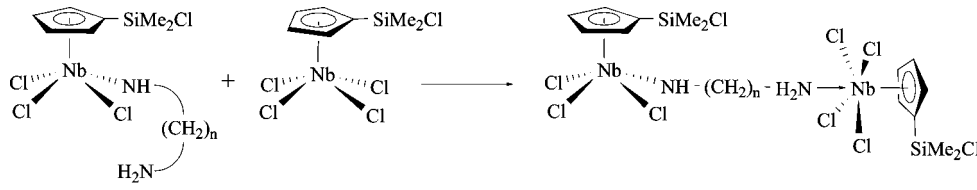

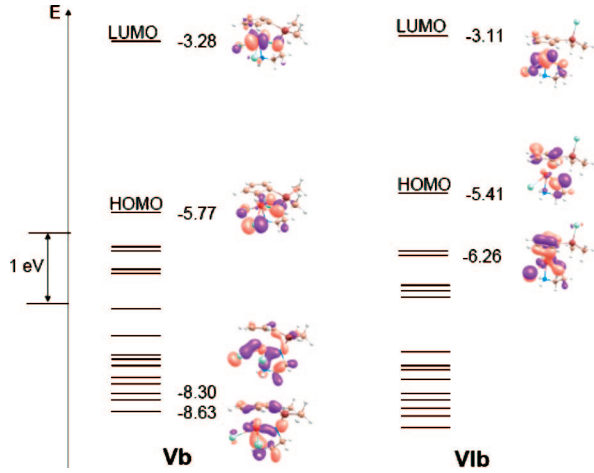

Figure 4. Frontier orbital diagram for complexes **Vb** and **VIb.**

Table 3. Natural Charges (au) for Various Complexes

	Ia	IIb	IVb	Vb	VIb
Si	1.668	1.676	1.681	1.873	1.676
Δ(Si)[a]	0.000	0.008	0.013	0.205	0.008
C_{ipso}	−0.622	−0.634	−0.591	−0.543	−0.608
Δ(C_{ipso})[a]	0.000	0.011	0.031	0.079	0.014

[a] Relative to **Ia**.

energy to the HOMO and about 0.8 eV lower in energy, we find a Nb−N π-bonding orbital. In contrast, for compound **Vb** with a N−Si bond, the HOMO/LUMO set represents the Nb−N π-bonding and π-antibonding orbitals. The former lone pair π-orbital of the amido nitrogen now participates in a σ-bonding interaction with the silicon center of the silyl group and also shows some bonding interaction with the *ipso*-C atom of the cyclopentadienyl ring. These orbitals are about 2.5 eV lower in energy than the HOMO.

The primary N−Si and the secondary N−C_{ipso} interactions as seen in the frontier orbital diagram also affect the electron density at Si and C. The more electronegative N-atom causes charge depletion at silicon and at the *ipso* carbon atom. These considerations provide a qualitative basis for a prediction of trends to be observed in ^{13}C NMR. We have established the chemical shifts of the resonance due to the cyclopentadienyl *ipso*-carbon atom observed in the ^{13}C NMR spectra and the silicon resonances in the ^{29}Si NMR spectra as definitive NMR features to distinguish the cyclopentadienyl-silyl-amido or imido nature of **3** and **4**, respectively. A charge analysis should provide an explanation for the features as detected by NMR spectroscopy.

Natural charges at Si and C obtained from a natural bond analysis are collected in Table 3. If we compare the CGC complex **Vb** with other amido or imido complexes without N−Si linkage, we see that this compound has significantly less charge not only on Si but on C_{ipso} as well. This charge depletion then provides a first argument for the fact that for **Vb** a significant highfield shifted NMR signal is observed for the *ipso*-carbon ^{13}C resonance and the ^{29}Si resonance.

Discussion

According to the experimental findings[26,30–32,36] and the results obtained by the computational chemistry study using DFT calculations, we suggest that the reaction of [Nb(η⁵-$C_5H_4SiMe_2Cl$)Cl_4] with diamines is initiated by the coordination of the diamine to the niobium center, through the highest protonated amine end, giving the intermediate adduct (**A**) (Scheme 12) (dinuclear adducts **6** showing this type of coordination have been isolated). Subsequent aminolysis of one of the Nb−Cl bonds renders the corresponding amido transient (**B**). As deduced from theoretical study, such a transformation constitutes an endothermic reaction, and therefore it is proposed that the thermodynamic driving force for this reaction is the formation of the insoluble ammonium chloride salt.

From the amido transient species **B**, the process may follow two different pathways depending on the ability of the additional amine functionality tethered to the amido nitrogen to coordinate in an intramolecular manner. Under conditions in which the pendant amine functionality is unable to coordinate, the reaction goes through the cleavage of a further Nb−Cl bond as the process is thermodynamically more favored, giving the corresponding imido derivative. In contrast, coordination of the pendant amine end to niobium to form the amido-amine intermediate (**C**) induces an energetic preference for the cleavage of the Si−Cl bond and formation of a cyclopentadienyl-silyl-amido complex.

As inferred from the theoretical study, the energetic gain caused by additional intramolecular donor stabilization is not exclusive for cyclopentadienyl-silyl-amido complexes, but rather imido derivatives also undergo additional donor interactions. Nevertheless, the fact that the amine group is tethered to the Nb−N (amido or imido) nitrogen atom, a situation that involves no drawbacks for cyclopentadienyl-silyl-amido derivatives, with the imido species imposes a distortion in the coordination geometry of the imido nitrogen and a marked weakening of the Nb−N(imido) interaction together with a weaker donating interaction from the amine group, showing that the imido complexes are not stabilized by an additional coordination of the pendant amine group.

Concluding Remarks

We have developed a simple and versatile synthetic approach to prepare a wide range of niobium complexes that include both mono- and dinuclear derivatives. Thus, new cyclopentadienyl-silyl-amido-amine derivatives [Nb{η⁵-$C_5H_4SiMe_2$-η-$N(CH_2)_3$-NHR}Cl_3] (R = H, **3a**; Me, **3b**), imido species [Nb(η⁵-$C_5H_4SiMe_2Cl$){$N(CH_2)_3$NMeR}Cl_2] (R = Me, **4a**; H, **4b**), an amido-amine compound [Nb(η⁵-$C_5H_4SiMe_2Cl$)(NMe$(CH_2)_2$-η-NHMe)Cl_3] (**7**), bridged-diimido species [{Nb(η⁵-$C_5H_4SiMe_2Cl$)-Cl_2}$_2${μ-$N(CH_2)_n$-η-N}] (n = 3, **5a**; 4, **5b**; 5, **5c**), and diamine adducts [{Nb(η⁵-$C_5H_4SiMe_2Cl$)Cl_4}$_2${μ-$NH_2(CH_2)_n$-η-NH_2}] (n = 3, **6a**; 4, **6b**; 5, **6c**) have been reported. The formation of these species involves different reaction pathways. Computational chemistry study using DFT calculations has permitted us to propose the reaction pathway followed by these reactions, which established the most favorable working conditions to selectively prepare the different types of complex obtained by reaction of [Nb(η⁵-$C_5H_4SiMe_2Cl$)Cl_4] with different diamines. In addition, as deduced from this study, the highfield shift of the resonance due to the cyclopentadienyl *ipso*-carbon atom and the silicon atom results from the presence of primary N−Si and secondary N−C_{ipso} bonding interactions, and CGCs show charge depletion at the silicon and *ipso*-carbon centers. The structures of [Nb{η⁵-$C_5H_4SiMe_2$-η-$N(CH_2)_2$-η-NMe_2}Cl_3] and [{Nb(η⁵-$C_5H_4SiMe_2Cl$)Cl_4}$_2${μ-$NH_2(CH_2)_3$-η-NH_2}] were determined by X-ray diffraction methods.

Experimental Section

General Considerations. All manipulations were performed under argon using Schlenk and high-vacuum line techniques or in

Scheme 12

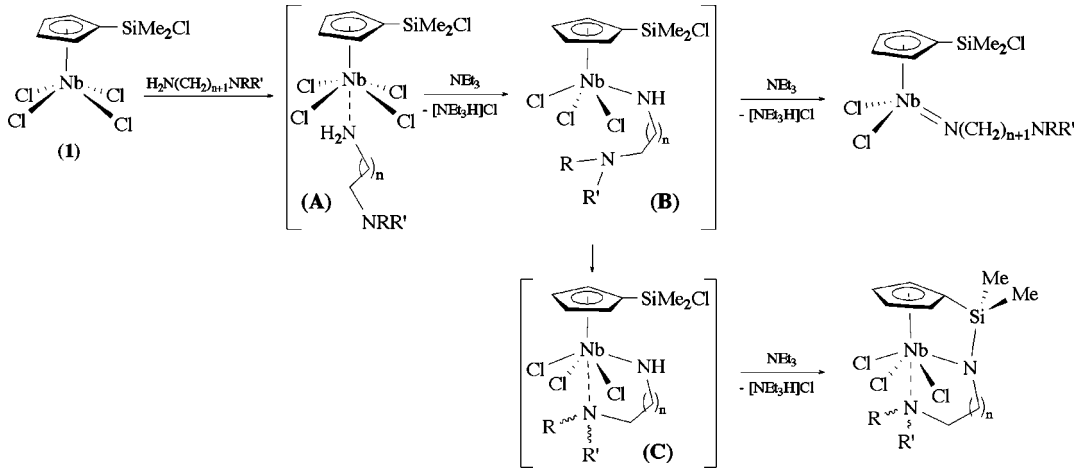

a glovebox model HE-63. The solvents were purified by distillation under argon before use by employing the appropriate drying/deoxygenated agent. Deuterated solvents were stored over activated 4 Å molecular sieves and degassed by several freeze–thaw cycles. NEt_3 (Aldrich) was distilled before use and stored over 4 Å molecular sieves. Diamines (Aldrich) were purchased from commercial sources and used without further purification. [Nb(η^5-$C_5H_4SiMe_2Cl$)Cl_4][32] was prepared by a known procedure. C, H, and N microanalyses were performed on a Perkin-Elmer 240B and/or Heraeus CHN-O-Rapid microanalyzer. NMR spectra measured at 25 °C were recorded on a Bruker AV400 (^{1}H NMR at 400 MHz, ^{13}C NMR at 100.6 MHz, ^{29}Si NMR at 79.5 MHz) spectrometer, and chemical shifts are referenced to residual solvent protons. BP86 density functional calculations have been carried out with the Gaussian03 program system. Computational details and full references are given in Supporting Information.

Synthesis of [Nb{η^5-$C_5H_4SiMe_2$-η-$N(CH_2)_3$-η-NHMe}Cl_3] (3b). A toluene solution (10 mL) of $NH_2(CH_2)_3NHMe$ (0.13 mL, 1.27 mmol) and NEt_3 (0.35 mL, 2.54 mmol) was added to a dark red solution of [Nb(η^5-$C_5H_4SiMe_2Cl$)Cl_4] (0.50 g, 1.27 mmol) in toluene (30 mL) at room temperature. The color of the reaction mixture immediately changed to greenish orange. The reaction mixture was stirred for 2 h, the white solid formed was collected by filtration, and the volatiles were removed under vacuum. The residue was washed with *n*-hexane (30 mL) and extracted into toluene (2 × 20 mL). The resulting solution was concentrated to ca. half-volume and cooled to −20 °C to afford **3b** in 80.3% yield (0.41 g, 1.02 mmol). Anal. Calcd for $C_{11}H_{20}Cl_3N_2NbSi$: C, 32.25; H, 4.93; N, 6.83. Found: C, 32.39; H, 4.53; N, 6.80. ^{1}H NMR (400 MHz, C_6D_6): δ −0.01, 0.00 (s, 2 × 3H, $SiMe_2$), 1.08, 1.74, 2.14, 2.90, 3.23, 3.39 (m, 6 × 1H, CH_2), 2.77 (d, J = 6.2 Hz, 3H, NH*Me*), 4.71 (brm, 1H, N*H*Me), 6.66, 6.74, 6.77, 6.90 (ABCD spin system, 4 × 1H, C_5H_4). ^{13}C{^{1}H} NMR (100.6 MHz, C_6D_6): δ −5.2, −5.1 ($SiMe_2$), 24.0, 41.9, 55.5 (CH_2), 49.6 (NHMe), 106.6 (C_5H_4-*ipso*), 126.2, 126.6, 127.3, 128.9 (C_5H_4). ^{29}Si NMR (79.5 MHz, C_6D_6): δ −11.9 (*Si*Me_2).

Synthesis of [Nb(η^5-$C_5H_4SiMe_2Cl$){$N(CH_2)_3NMe_2$}Cl_2] (4a). A method similar to that described for **3b** was adopted by using $NH_2(CH_2)_3NMe_2$ (0.16 mL, 1.27 mmol) to give **4a** as a green solid. Yield: 73% (0.39 g, 0.93 mmol). Anal. Calcd for $C_{12}H_{22}Cl_3N_2NbSi$: C, 34.01; H, 5.24; N, 6.60. Found: C, 34.22; H, 5.10; N, 6.63. ^{1}H NMR (400 MHz, C_6D_6): δ 0.57 (s, 6H, $SiMe_2$), 1.47, 2.29, 3.78 (brm, 3 × 2H, CH_2), 2.02 (brs, 6H, NMe_2), 6.01, 6.36 (AA′BB′ spin system, 2 × 2H, C_5H_4). ^{13}C{^{1}H} NMR (100.6 MHz, $CDCl_3$): δ 1.3 ($SiMe_2$), 28.0, 57.6, 63.7 (CH_2), 45.7 (NMe_2), 114.4, 122.8 (C_5H_4), 128.0 (C_5H_4-*ipso*). ^{29}Si NMR (79.5 MHz, C_6D_6): δ 15.3 (*Si*Me_2).

Synthesis of [Nb(η^5-$C_5H_4SiMe_2Cl$){$N(CH_2)_3NHMe$}Cl_2] (4b). A solution of $NH_2(CH_2)_3NHMe$ (0.40 mL, 3.83 mmol) in toluene (10 mL) was added to a solution of [Nb(η^5-$C_5H_4SiMe_2Cl$)Cl_4] (0.50 g, 1.27 mmol) in toluene (30 mL). The mixture quickly became cloudy, and the reaction mixture was stirred for 3 h. The solid formed was collected by filtration, and volatiles were completely removed under reduced pressure. The residue was extracted into toluene (3 × 10 mL), and the resulting solution was concentrated to ca. half-volume and cooled to −20 °C to afford **4b**, which was recrystallized from a cold toluene/hexane mixture. Yield: 65.8% (0.34 g, 0.83 mmol). Anal. Calcd for $C_{11}H_{20}Cl_3N_2NbSi$: C, 32.25; H, 4.93; N, 6.83. Found: C, 32.19; H, 4.73; N, 7.10. ^{1}H NMR (400 MHz, C_6D_6): δ 0.63 (s, 6H, $SiMe_2$), 0.90 (brm, 1H, N*H*Me), 1.91, 2.77, 3.77 (brm, 3 × 2H, CH_2), 2.34 (brs, 3H, NH *Me*), 6.36, 6.58 (AA′BB′ spin system, 2 × 2H, C_5H_4). ^{13}C{^{1}H} NMR (100.6 MHz, C_6D_6): δ 2.5 ($SiMe_2$), 29.8, 59.7, 63.9 (CH_2), 48.5 (NHMe), 114.7, 123.6 (C_5H_4), C_5H_4-*ipso* resonance is underneath the solvent signals. ^{29}Si NMR (79.5 MHz, C_6D_6): δ 16.0 (*Si*Me_2).

Synthesis of [{Nb(η^5-$C_5H_4SiMe_2Cl$)Cl_2}$_2${μ-*N*-$(CH_2)_3$-η-N}] (5a). A mixture of $NH_2(CH_2)_3NH_2$ (0.03 mL, 0.32 mmol) and NEt_3 (0.18 mL, 1.28 mmol) in toluene (10 mL) was added to a stirred solution of [Nb(η^5-$C_5H_4SiMe_2Cl$)Cl_4] (0.25 g, 0.64 mmol) in toluene (20 mL) at room temperature. After the reaction mixture was stirred for 2 h, the solid formed was collected by filtration, and the solution was concentrated (20 mL) and cooled to −20 °C to afford **5a** as a yellow solid, which was recrystallized from a cold toluene/hexane mixture. Yield: 52.2% (0.12 g, 0.17 mmol). Anal. Calcd for $C_{17}H_{26}Cl_6N_2Nb_2Si_2$: C, 28.63; H, 3.68; N, 3.92. Found: C, 28.44; H, 3.93; N, 3.71. ^{1}H NMR (400 MHz, C_6D_6): δ 0.56 (s, 12H, $SiMe_2$), 1.37, 3.97 (m, 2H, 4H, CH_2), 6.08, 6.36 (AA′BB′ spin system, 2 × 4H, C_5H_4). ^{13}C{^{1}H} NMR (100.6 MHz, $CDCl_3$): δ 2.9 ($SiMe_2$), 33.9, 63.3 (CH_2), 114.6, 122.3 (C_5H_4), C_5H_4-*ipso* resonance is underneath the solvent signals. ^{29}Si NMR (79.5 MHz, $CDCl_3$): δ 15.9 (*Si*Me_2).

Synthesis of [{Nb(η^5-$C_5H_4SiMe_2Cl$)Cl_2}$_2${μ-*N*-$(CH_2)_4$-η-N}] (5b). A method similar to that used for **5a** was adopted by using $NH_2(CH_2)_4NH_2$ (0.03 mL, 0.32 mmol) to give **5b**. Yield: 60.6% (0.14 g, 0.19 mmol). Anal. Calcd for $C_{18}H_{28}Cl_6N_2Nb_2Si_2$: C, 29.73; H, 3.89; N, 3.85. Found: C, 29.50; H, 4.23; N, 3.80. ^{1}H NMR (400 MHz, C_6D_6): δ 0.55 (s, 12H, $SiMe_2$), 1.52, 3.64 (m, 2 × 4H, CH_2), 6.01, 6.34 (AA′BB′ spin system, 2 × 4H, C_5H_4). ^{13}C{^{1}H} NMR (100.6 MHz, C_6D_6): δ 2.6 ($SiMe_2$), 29.5, 66.1 (CH_2), 114.2, 121.8 (C_5H_4), C_5H_4-*ipso* resonance is underneath the solvent signals. ^{29}Si NMR (79.5 MHz, C_6D_6): δ 16.0 (*Si*Me_2).

Synthesis of [{Nb(η^5-$C_5H_4SiMe_2Cl$)Cl_2}$_2${μ-*N*-$(CH_2)_5$-η-N}] (5c). A method similar to that used for **5a** was adopted by using $NH_2(CH_2)_5NH_2$ (0.04 mL, 0.32 mmol) to give **5c**. Yield: 63.7% (0.15, 0.20 mmol). Anal. Calcd for $C_{19}H_{30}Cl_6N_2Nb_2Si_2$: C, 30.79; H, 4.09; N, 3.78. Found: C, 30.54; H, 4.40, N, 3.81. ^{1}H NMR (400 MHz, C_6D_6): δ 0.54 (s, 12H, $SiMe_2$), 1.36, 1.44, 3.65 (m, 4H, 2H, 4H, CH_2), 5.96, 6.32 (AA′BB′ spin system, 2 × 4H, C_5H_4). ^{13}C{^{1}H}

NMR (100.6 MHz, C_6D_6): δ 2.6 ($SiMe_2$), 24.7, 31.3, 66.7 (CH_2), 114.3, 121.6 (C_5H_4), the C_5H_4-*ipso* resonance is underneath the solvent signals. ^{29}Si NMR (79.5 MHz, C_6D_6): δ 15.9 (*Si*Me_2).

Synthesis of [{Nb(η⁵-C₅H₄SiMe₂Cl)Cl₄}₂{μ-NH₂-(CH₂)₃-η-NH₂}] (6a). A toluene solution (10 mL) of $NH_2(CH_2)_3NH_2$ (0.07 mL, 0.84 mmol) was added to a dark red solution of [Nb(η⁵-$C_5H_4SiMe_2Cl)Cl_4$] (0.25 g, 0.64 mmol) in toluene (20 mL) at room temperature. The color of the reaction mixture immediately changed to red, a white solid was formed, and stirring was continued for further 2 h. The reaction mixture was filtered, and the solution was concentrated (10 mL) and cooled to −20 °C to afford **6a** as an red solid, which was recrystallized from a cold toluene/hexane mixture. Yield: 40.1% (0.11, 0.13 mmol). Anal. Calcd for $C_{17}H_{30}Cl_{10}N_2Nb_2Si_2$: C, 23.77; H, 3.53; N, 3.26. Found: C, 24.08; H, 3.88, N, 3.68. ^{1}H NMR (400 MHz, C_6D_6): δ 0.77 (s, 12H, $SiMe_2$), 0.26, 3.01 (m, 2H, 4H, CH_2), 4.62 (brm, 4H, NH_2), 6.64, 6.66 (AA′BB′ spin system, 2 × 4H, C_5H_4). ^{13}C{^{1}H} NMR (100.6 MHz, C_6D_6): δ 2.7 ($SiMe_2$), 30.4, 42.7 (CH_2), 132.0, 132.5 (C_5H_4), 136.3 (C_5H_4-*ipso*). ^{29}Si NMR (79.5 MHz, C_6D_6): δ 14.8 (*Si*Me_2).

Synthesis of [{Nb(η⁵-C₅H₄SiMe₂Cl)Cl₄}₂{μ-NH₂-(CH₂)₄-η-NH₂}] (6b). This product was prepared as described above for **6a** by using $NH_2(CH_2)_4NH_2$ (0.09 mL, 0.89 mmol) to give **6b**. Yield: 43.3% (0.12 g, 0.14 mmol). Anal. Calcd for $C_{18}H_{32}Cl_{10}N_2Nb_2Si_2$: C, 24.76; H, 3.70; N, 3.20. Found: C, 24.52; H, 4.19, N, 3.66. H NMR (400 MHz, C_6D_6): δ 0.78 (s, 12H, $2SiMe_2$), 0.42, 3.05 (brm, 2 × 4H, CH_2), 4.63 (brm, 4H, NH_2), 6.68, 6.70 (AA′BB′ spin system, 2 × 4H, C_5H_4). ^{13}C{^{1}H} NMR (100.6 MHz, C_6D_6): δ 2.8 ($SiMe_2$), 29.2, 45.6 (CH_2), 132.1, 132.5 (C_5H_4), 136.3 (C_5H_4-*ipso*). ^{29}Si NMR (79.5 MHz, C_6D_6): δ 14.9 (*Si*Me_2).

Synthesis of [{Nb(η⁵-C₅H₄SiMe₂Cl)Cl₄}₂{μ-NH₂-(CH₂)₅-η-NH₂}] (6c). This product was prepared as described above for **6a** by using $NH_2(CH_2)_5NH_2$ (0.10 mL, 0.85 mmol) to give **6c** as a green solid. Yield: 39% (0.11 g, 0.125 mmol). Anal. Calcd for $C_{19}H_{34}Cl_{10}N_2Nb_2Si_2$: C, 25.72; H, 3.87; N, 3.15. Found: C, 25.48; H, 4.20, N, 3.80. ^{1}H NMR (400 MHz, C_6D_6): δ 0.78 (s, 12H, $SiMe_2$), 0.55, 0.63, 3.16 (m, 2H, 2 × 4H, CH_2), 4.76 (m, 2H, NH_2), 6.67, 6.69 (AA′BB′ spin system, 2 × 4H, C_5H_4). ^{13}C{^{1}H} NMR (100.6 MHz, C_6D_6): δ 2.7 ($SiMe_2$), 23.6, 31.9, 45.6 (CH_2), 132.1, 132.5 (C_5H_4), 136.3 (C_5H_4-*ipso*). ^{29}Si NMR (79.5 MHz, C_6D_6): δ 14.8 (*Si*Me_2).

Synthesis of [Nb(η⁵-C₅H₄SiMe₂Cl){NMe-(CH₂)₂-η-NHMe}Cl₃] (7). A toluene solution (10 mL) of $NHMe(CH_2)_2NHMe$ (0.14 mL, 1.31 mmol) and NEt_3 (0.35 mL, 2.54 mmol) was added to a toluene solution of **1** (0.50 g, 1.27 mmol) at room temperature. After stirring for 3 h, the solution was filtered, and volatiles were completely removed. The residue was washed with *n*-hexane (30 mL) and extracted into toluene (2 × 20 mL). The resulting solution was concentrated (15 mL) and cooled to −20 °C to afford **7** as a red crystalline solid in 72.5% yield (0.41 g, 0.92 mmol). Anal. Calcd for $C_{11}H_{21}Cl_4N_2NbSi$: C, 29.75; H, 4.77; N, 6.30. Found: C, 30.24; H, 4.40, N, 5.91. ^{1}H NMR (400 MHz, C_6D_6): δ 1.00, 1.01 (s, 2 × 3H, $SiMe_2$), 2.38, 2.76, 3.06, 3.27 (m, 4 × 1H, CH_2), 2.75 (d, J = 4.8 Hz, 3H, NH*Me*), 2.99 (3H, NMe), 5.93, 5.97, 6.45, 6.53 (ABCD spin system, 4 × 1H, C_5H_4). ^{13}C{^{1}H} NMR (100.6 MHz, C_6D_6): δ 1.1 ($SiMe_2$), 40.1 (NHMe), 50.9, 67.3 (CH_2), 58.0 (NMe), 117.9, 118.9, 125.8, 125.9 (C_5H_4), C_5H_4-*ipso* resonance is underneath the solvent signals. ^{29}Si NMR (79.5 MHz, C_6D_6): δ 14.5 (*Si*Me_2).

Single-Crystal X-ray Structure Determination of Compounds 2c and 6b. Crystal data and details of the structure determination are presented in Table 4. Suitable single crystals of **2c** and **6b** for the X-ray diffraction study were selected, covered with perfluorinated ether and mounted on a Bruker-Nonius Kappa CCD single crystal diffractometer equipped with a graphite-monochromated Mo Kα radiation (λ = 0.71073 Å). Data collection was performed at 200(2) K. Multiscan[50] absorption correction procedures were applied to the data. The structures were solved, using the WINGX package,[51] by direct methods (SHELXS-97) and refined by using full-matrix least-squares against F^2 (SHELXL-97).[52] All nonhydrogen atoms were anisotropically refined. Hydrogen atoms were geometrically placed and left riding on their parent atoms. For **2c** the particular crystal studied proved to be a racemic twin and was refined using the TWIN and BASF instructions, resulting in a 38:62 components ratio. Full-matrix least-squares refinements were carried out by minimizing $\Sigma\, w(F_0^2 - F_c^2)^2$ with the SHELXL-97 weighting scheme and stopped at shift/err <0.001. The final residual electron density maps showed no remarkable features.

Table 4. Crystallographic Data for 2c and 6b

	2c	**6b·2(C₇H₈)**
formula	$C_{11}H_{20}Cl_3N_2NbSi$	$C_{32}H_{48}Cl_{10}N_2Nb_2Si_2$
FW	407.64	1057.22
color/habit	yellow/prism	red/prism
crystal dimensions, mm³	0.35 × 0.20 × 0.19	0.42 × 0.34 × 0.32
crystal syst	orthorhombic	triclinic
space group	$Pna2_1$	$P\bar{1}$
a, Å	14.5718(14)	7.1260(5)
b, Å	9.8872(17)	12.059(2)
c, Å	11.2689(18)	13.190(2)
α, deg	90	88.892(15)
β, deg	90	83.721(12)
γ, deg	90	87.827(10)
V, Å³	1623.6(4)	1125.7(3)
Z	4	1
T, K	200	200
D_{calcd}, g cm^{-3}	1.668	1.560
μ, mm^{-1}	1.294	1.181
F(000)	824	534
θ range, deg	3.33 - 27.51	3.11 to 27.50
Index ranges (h, k, l)	±18, ±12, ±14	±9, ±15, ±17
no. of rflns collected	34587	20516
no. of indep rflns/R_{int}	3713/0.0509	5116/0.0286
no. of obsd rflns ($I > 2\sigma(I)$)	2853	4046
no. of data/restraints/params	3713/1/164	5116/0/217
$R1$/$wR2$ ($I > 2\sigma(I)$)[a]	0.0300/0.0668	0.0376/0.0857
$R1$/$wR2$ (all data)[a]	0.0499/0.0731	0.0586/ 0.0970
GOF (on F^2)[a]	1.007	1.049
largest diff peak and hole (e Å^{-3})	+0.531/−0.481	+1.226/−1.050

[a] $R1 = \Sigma(||F_0| - |F_c||)/\Sigma|F_o|$; $wR2 = \{\Sigma[\, w(F_0^2 - F_c^2)^2]/\Sigma[w(F_0^2)^2]\}^{1/2}$; GOF = $\{\Sigma[\, w(F_0^2 - F_c^2)^2]/(n-p)\}^{1/2}$.

Acknowledgment. Financial support for this research by DGICYT (Project MAT2007-60997) and C.A.M (Project GR/MAT/0622/2004) is gratefully acknowledged. M.C.M acknowledges Universidad de Alcalá for fellowships. We gratefully acknowledge Prof. L. Cavallo for granting access to the MoLNaC Computing Facilities at Dipartimento di Chimica, Univertità di Salerno.

Supporting Information Available: Tables of crystallographic data, including fractional coordinates, bond lengths and angles, anisotropic displacement parameters, and hydrogen atom coordinates in CIF format of complexes **3b** and **6b·2(C₇H₈)**. Computational details, Cartesian coordinates and final energies for optimized complexes. This material is available free of charge via the Internet at http://pubs.acs.org.

OM701003T

(50) Blessing, R. H. SORTA V. *Acta Crystallogr., Sect. A* **1995**, *51*, 33–38.
(51) Farrugia, L. J. *J. Appl. Crystallogr.* **1999**, *32*, 837–938.
(52) Sheldrick, G. M. SHELXL-97; Universität Göttingen: Göttingen, Germany, 1998.